Measuring Fluctuating Pressure Levels and Vibration Response in a Jet Plume

Douglas J. Osterholt
Douglas M. Knox
ATA Engineering, Inc., San Diego, California

ABSTRACT

The characterization of loads due to solid rocket motor plume impingement allows for more-accurate analyses of components subjected to such an environment. Typically, test verification of predicted loads due to these conditions is widely overlooked or unsuccessful. ATA Engineering, Inc., performed testing during a solid rocket motor firing to obtain acceleration and pressure responses in the hydrodynamic field surrounding the jet plume. The test environment necessitated a robust design to facilitate measurements being made in close proximity to the jet plume. This paper presents the process of designing a test fixture and an instrumentation package that could withstand the solid rocket plume environment and protect the required instrumentation.

KEY WORDS: Fluctuating pressure, jet plume, vibration, accelerometer, pressure transducer, solid rocket motor, test

INTRODUCTION

The Orion crew module is a space exploration vehicle currently under development that will be used to launch astronauts into space. The Orion launch abort system (LAS) will allow the astronaut crew to escape in case of an emergency during launch. Current predictions show that when the solid rocket motors fire to launch the crew to safety, the loads induced on the crew module may damage its skins and/or be too loud for the crew. There are many unknowns in the analysis of the crew module skin—mainly due to loads caused by the plume impingement on the outer shell of the crew module.

In analysis-based predictions, the abort motor's plume-induced fluctuating pressure levels occurring during LAS abort separation are expected to exceed 175 dB, resulting in internal crew module component damage. The LAS crew module position relative to the plume from the LAS abort motor is shown in Figure 1 on the left; the figure on the right shows a previous test firing of the LAS abort motor. A large unknown in the analysis is the efficiency of the plume loads to drive vibration and vibroacoustic transmission of a structure. This test provided the opportunity to obtain test data characterizing the fluctuating pressures in the jet plume and the induced vibration of a steel panel. Further, this insight into the environment could be used to validate analytical methods to predict this behavior. The instrumentation panel was designed to measure fluctuating pressures both upstream and downstream of a vibration panel. The panel consisted of a 1/8"-thick steel plate on which accelerometers were mounted to measure the response due to the fluctuating pressures. The goal after the test was to show that analytical methods can be used to

predict the response of the panel and validate the methods while minimizing the uncertainty of analytical assumptions.

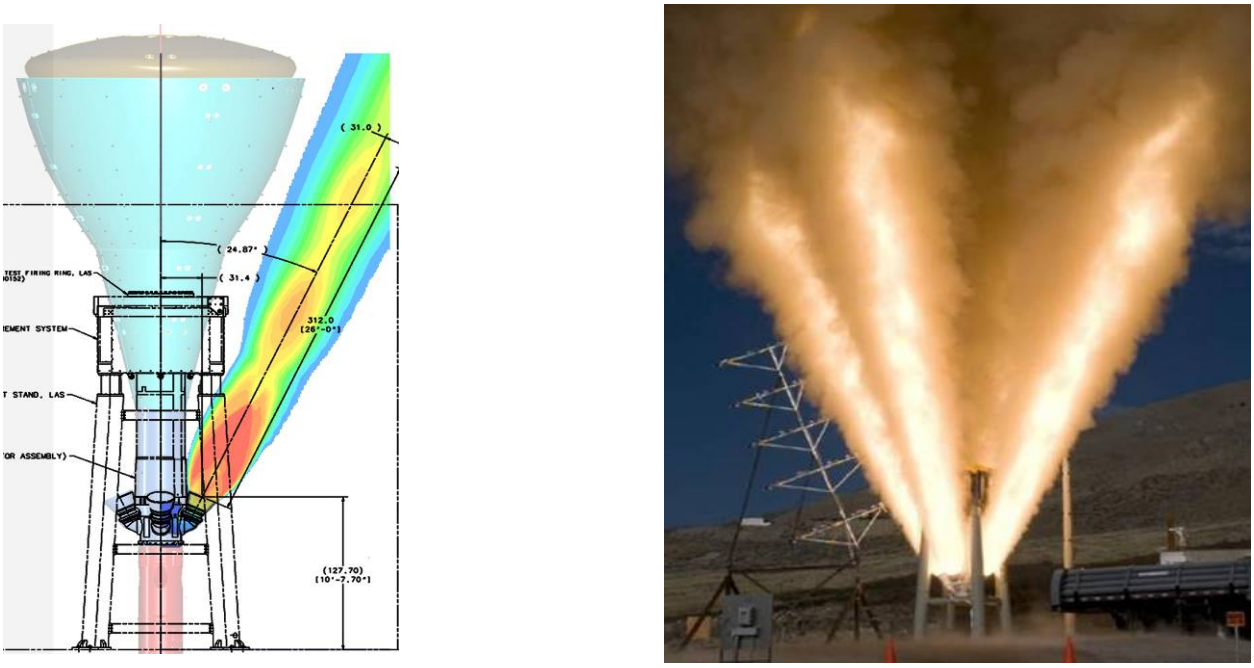

Figure 1. Abort motor plume position relative to the Orion CM and LAS (left) and photo of plumes during ST-1 static test firing (right).

ATA Engineering, Inc., (ATA) conducted a plume impingement aero-acoustic vibration (PIAAV) test in support of the Ascent Abort Plume Impingement Loads activity, the goal of which was to measure pressures at multiple points and the response of a thin panel. We designed a test panel that was installed on an existing structure and placed near the rocket plume during a solid rocket motor firing test performed on May 27, 2010. The panel test fixture was designed to hold and protect eleven pressure transducers and eight accelerometers. The main purpose of this paper is to describe how we successfully measured this data in the extreme environment of a jet plume. Although some data are presented, it is beyond the scope of this paper to present all of the data and analysis results.

In preparation for the test, ATA designed and built an instrumentation panel. NASA Marshall Space Flight Center (MSFC) provided a support table that was used to hold this panel. The instrumentation and measurement locations were selected based upon the temperatures and pressures predicted in the plume near-field. The radiant temperatures were estimated to be near 400 degrees F on the surface of the thin panel. Also considered was the potential for debris from the solid rocket motor to cause damage to transducers and cables. The final instrumentation package was selected from components readily available from suppliers in the limited time frame before the test. The vehicle used for this test was a 24”-diameter, single stage, solid rocket motor. Our test was added to a test that was already planned. This test firing was selected because of its similarities to the Orion Launch Abort System (LAS) in size, thrust, and duration of motor burn.

The remainder of this paper will discuss the test article, facility, instrumentation panel design, measurement locations, instrumentation used, test conduct, and some results of the test.

TEST ARTICLE AND FACILITY LAYOUT

The test vehicle was a 24”-diameter solid rocket motor with approximately a 14” nozzle exit diameter, 21,500 lb of thrust, and a 21-second burn. A model of the test area is shown in Figure 2. Testing was performed at the 24” motor test stand located at MSFC’s east test area in the solid propulsion test area (SPTA). Figure 3 shows a diagram of the expected jet plume and identifies its characteristics. The aero-acoustic near-field and hydrodynamic field were the areas of interest; the instrumentation panel was placed near the expected boundary of these two fields. The center of the instrumentation panel was installed approximately 60” downstream of the nozzle exit and 35” (approximately 2.5 nozzle diameters) radially outward from the nozzle center line, as shown in Figure 4.

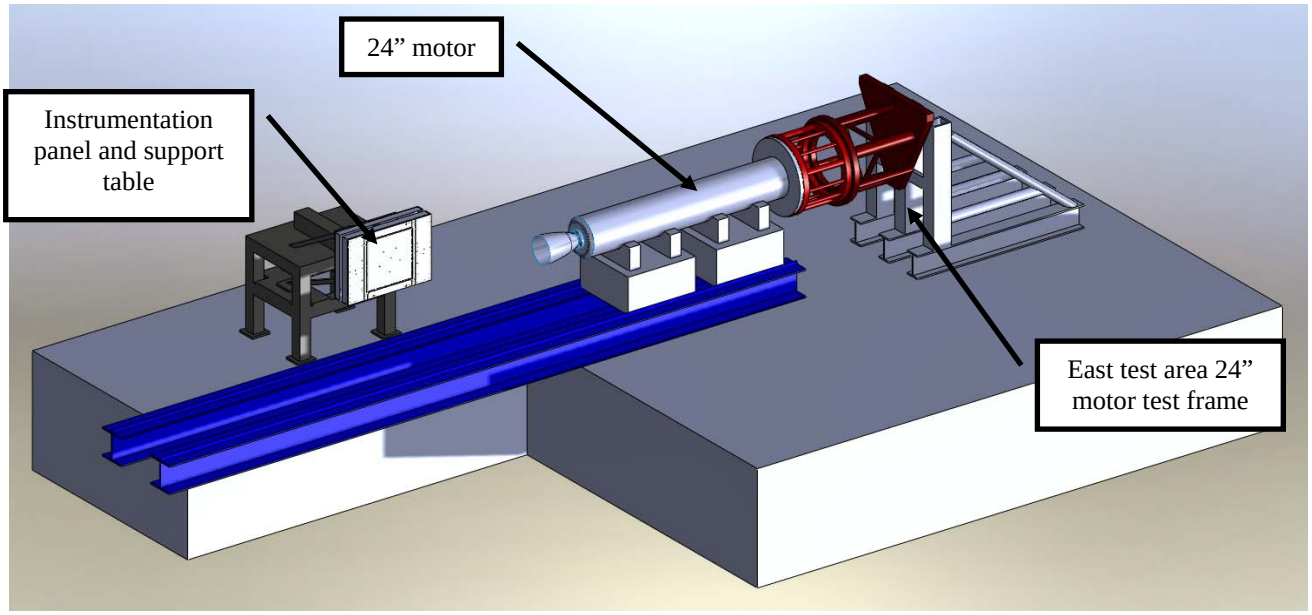

Figure 2. Overall view of 24” motor and SPTA test facility.

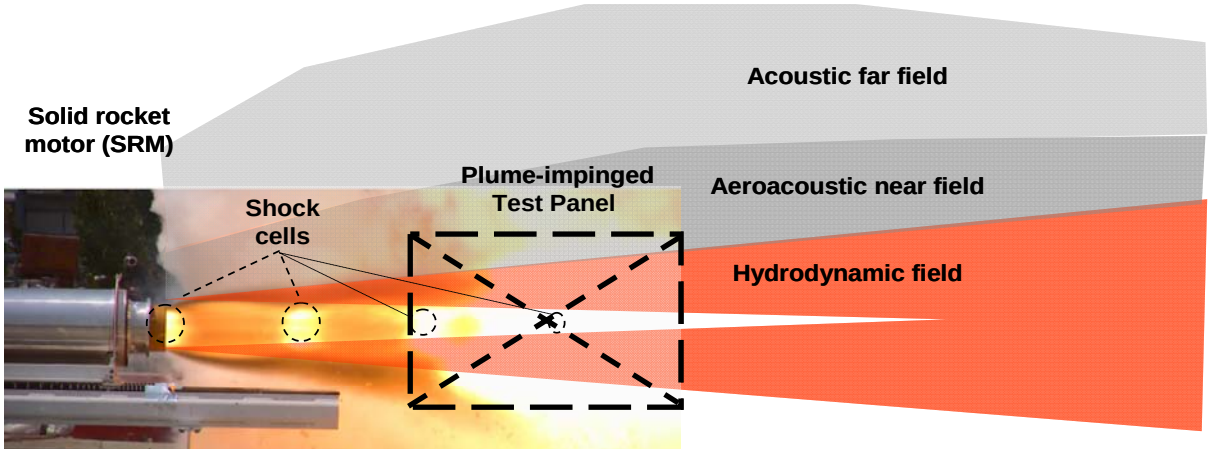

Figure 3. Solid rocket motor plume nomenclature.

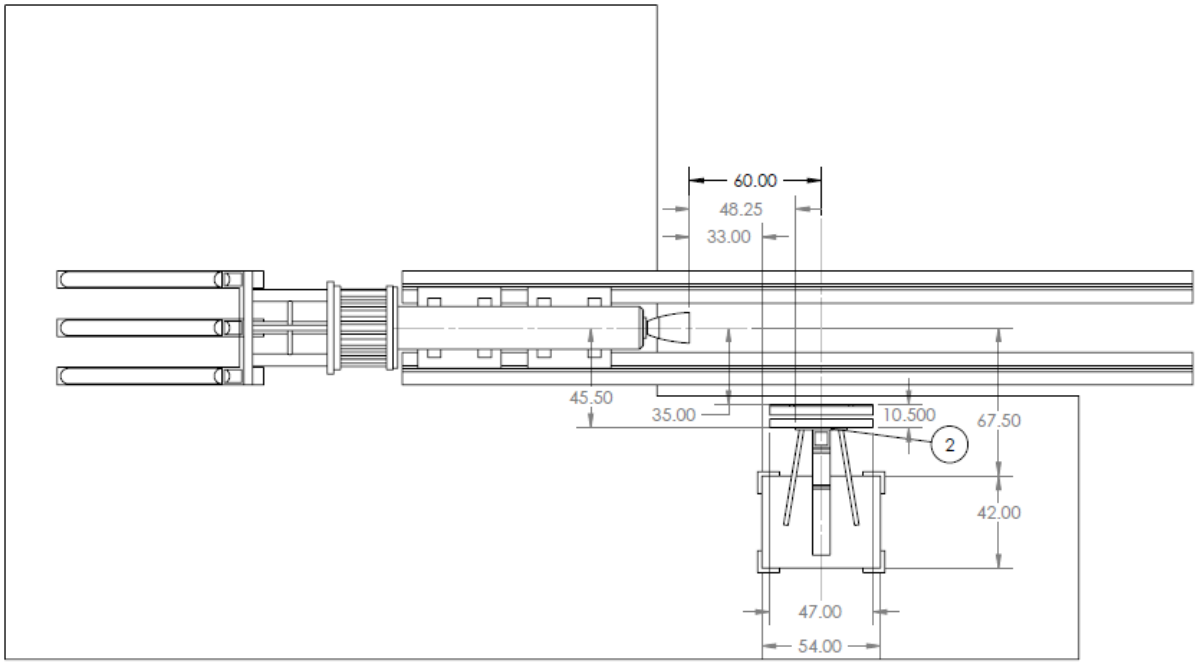

Figure 4. Instrumentation panel and support table location relative to the nozzle.

INSTRUMENTATION PANEL DESIGN

The design of the instrumentation panel was configured to be integrated with a support table, which was available from a previous test at MSFC. A photo of the support table that was previously used is shown in Figure 5. This provided a robust support and interface to hold the instrumentation.

Figure 5. Support table available from MSFC – bolted to the concrete pad.

The instrumentation panel consisted of three major components: the leading edge pressure plate, accelerometer vibration panel, and trailing edge pressure plate. These plates were all made of high-strength steel (T1 for the accelerometer panel and 4140 steel for pressure plates and accelerometer frame) bolted together and mounted to the support table. The sensor panels were bolted to the support table via steel unistrut channels, gussets, and brackets. A photo of the instrumentation panel showing the ¾”-thick steel plates used for the pressure panels and accelerometer panel support frame, airfoil, and 1/8”-thick steel accelerometer vibration panel is shown in Figure 6. Figure 7 shows the panels during installation and the unistrut support frame. The 1/8”-thick accelerometer panel is not shown installed in the picture but mounts in the open section shown.

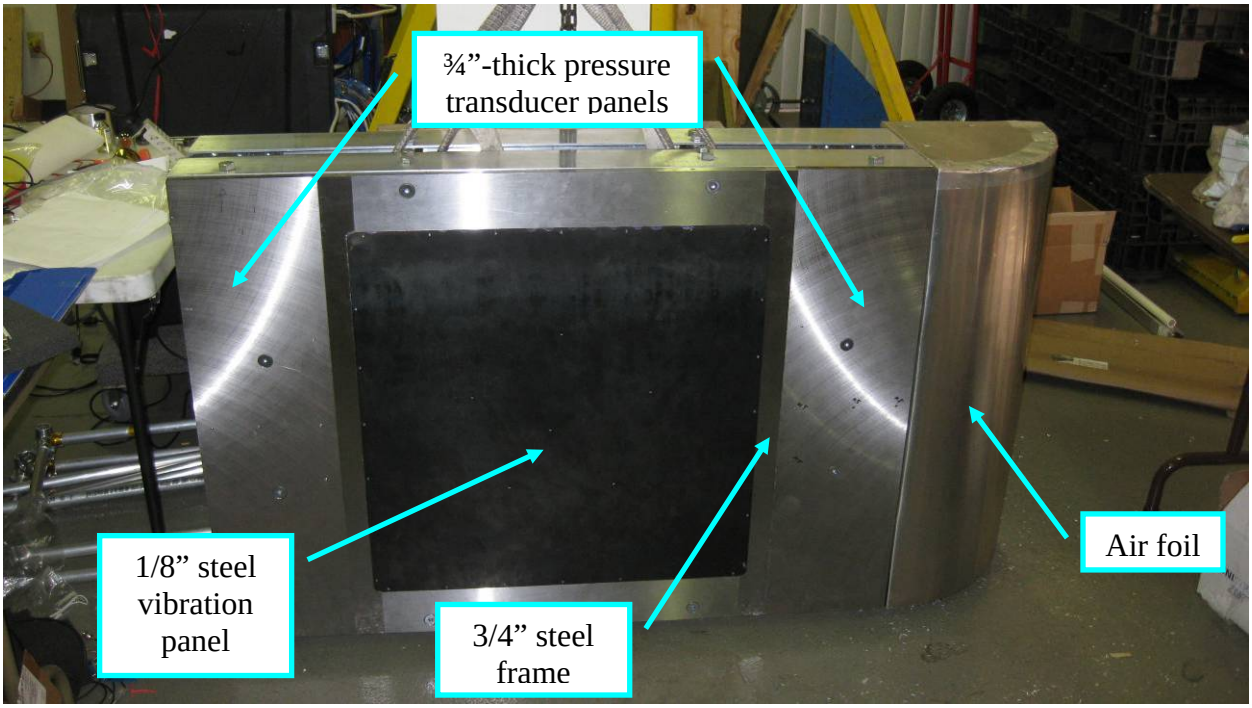

Figure 6. Instrumentation panel details.

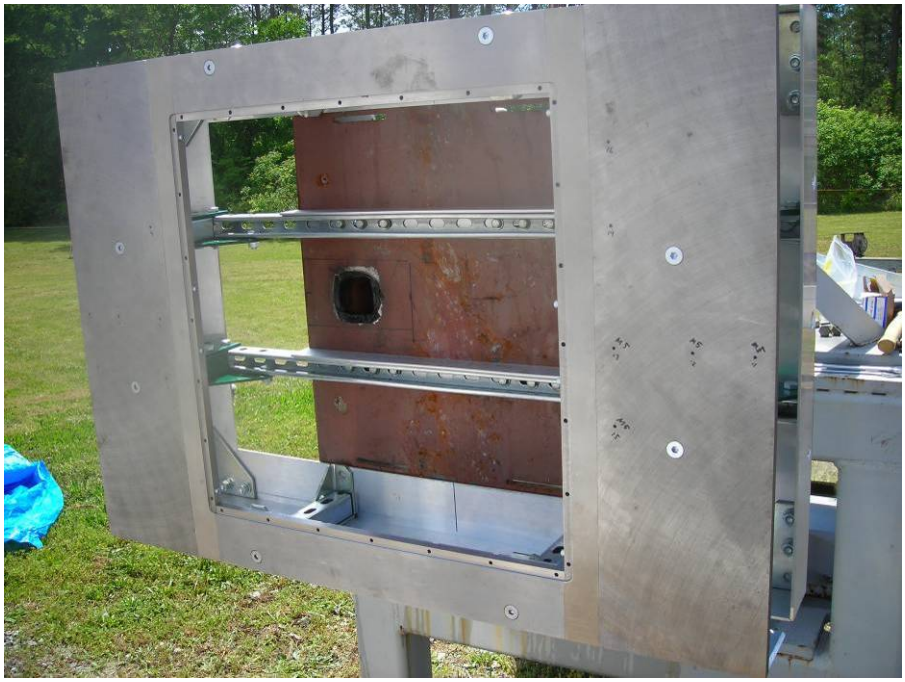

Figure 7. Steel unistrut supports bolting the instrumentation panel to the support table.

There was a concern that the leading edge of the panel would disrupt the flow of the plume and cause unwanted turbulence at the leading edge pressure panel. A semi-circular airfoil was designed and attached to the leading edge of the panel to minimize the turbulence and acoustic diffraction at the entry to the pressure plates. Another concern was that hot gases and pressures

would wrap around the panel and damage instrumentation cables on the back side. This could also affect the response by measuring the unwanted wrap-around pressures that could affect the response. To minimize this risk, close-out panels were added to prevent back pressure from wrapping around and influencing the measurements and to protect the instrumentation, as shown in Figure 8. We also installed a pressure transducer inside the box to characterize the amount of pressure leaking into the box. Acoustic damping internal to the box was also added to reduce reflected sound waves inside the box. The last concern was the heat from the plume melting the thin wall airfoil and the aluminum close-out panels on the top and bottom. To minimize this risk, thin sheets of self-adhesive cork were applied to the air foil and the top and bottom panels to protect the thin metal from the heat of the jet plume (Figure 9 and Figure 10). High-temperature tape was also used to seal the box frame. This helped prevent hot gases from entering the box and damaging cables.

Figure 8. Close-out panel on back side of box.

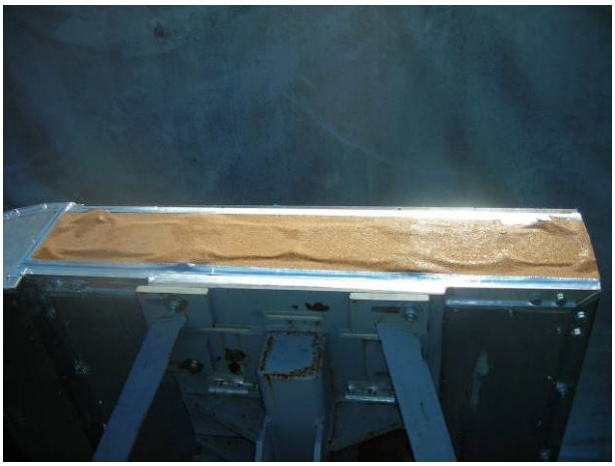

Figure 9. Thermal protection added to top and bottom panels (thin sheet of cork).

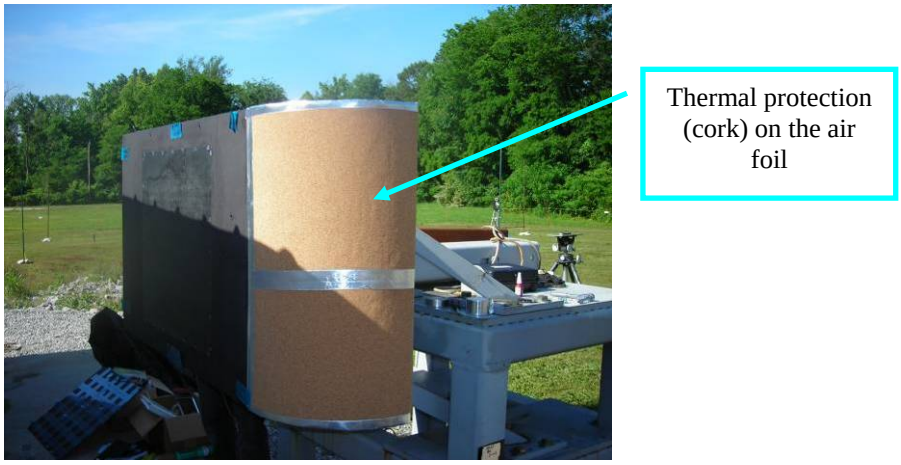

Figure 10. Thermal protection added to air foil (two layers of thin sheet cork).

MEASUREMENT LOCATIONS

The final set of measurement locations for the test included a total of twelve pressure transducers, eight accelerometers, and three thermocouples. Twenty-three total channels were measured for the motor firing test and are listed in Table 1.

The phase between the pressure transducers was important for predicting the loads. Because of this, the pressure transducers were placed 3", 4", and 6" apart from each other. The leading panel is symmetric to the aft panel, with the exception of one additional pressure transducer (P16). One accelerometer was placed on each pressure panel. Six accelerometers were placed in a pentagon shape on the 1/8" steel panel to measure as many modes of vibration as possible. One was just off the center of the panel. The accelerometer and pressure transducer locations are shown in Figure 11. The accelerometer locations were distributed on the 1/8"-thick panel to measure the overall vibration response.

Table 1. Instrumentation locations and channel list.

CH	SN	Node	DIR	Cal mV/EU	Channel Description	Data Type
1	P9396	17	X-	73.73	Inside box	Pressure
2	P9397	2	X-	72.37	Aft panel mid	Pressure
3	P9398	3	X-	73.36	Aft panel fwd	Pressure
4	P9399	4	X-	73.09	Aft panel top	Pressure
5	Q931	5	X-	73.52	Aft panel btm	Pressure
6	M9139	11	X-	50.44	Lead panel fwd	Pressure
7	M9140	12	X-	50.29	Lead panel mid	Pressure
8	M9142	13	X-	49.99	Lead panel aft	Pressure
9	M9143	15	X-	47.54	Lead panel btm	Pressure
10	Q932	14	X-	72.78	Lead panel top	Pressure
11	Q933	16	X-	73.65	Lead panel upper top	Pressure
12	L919	1	X-	73.55	Aft panel aft	Pressure
13	T1	1001	X+	1	Fwd pressure plate front surface	Temperature
14	T2	1002	X+	1	Fwd pressure plate back surface	Temperature
15	T3	1003	X+	1	Accel panel back	Temperature
16	30642	101	X+	9.38	Center	Accelerometer
17	30640	102	X+	9.08	Fwd center	Accelerometer
18	30543	103	X+	9.78	Fwd bottom	Accelerometer
19	30544	104	X+	9.55	Aft bottom	Accelerometer
20	30641	105	X+	9.31	Aft center	Accelerometer
21	30643	106	X+	9.46	Upper	Accelerometer
22	30639	107	X+	9.39	Lead pressure panel	Accelerometer
23	30653	108	X+	9.53	Aft pressure panel	Accelerometer

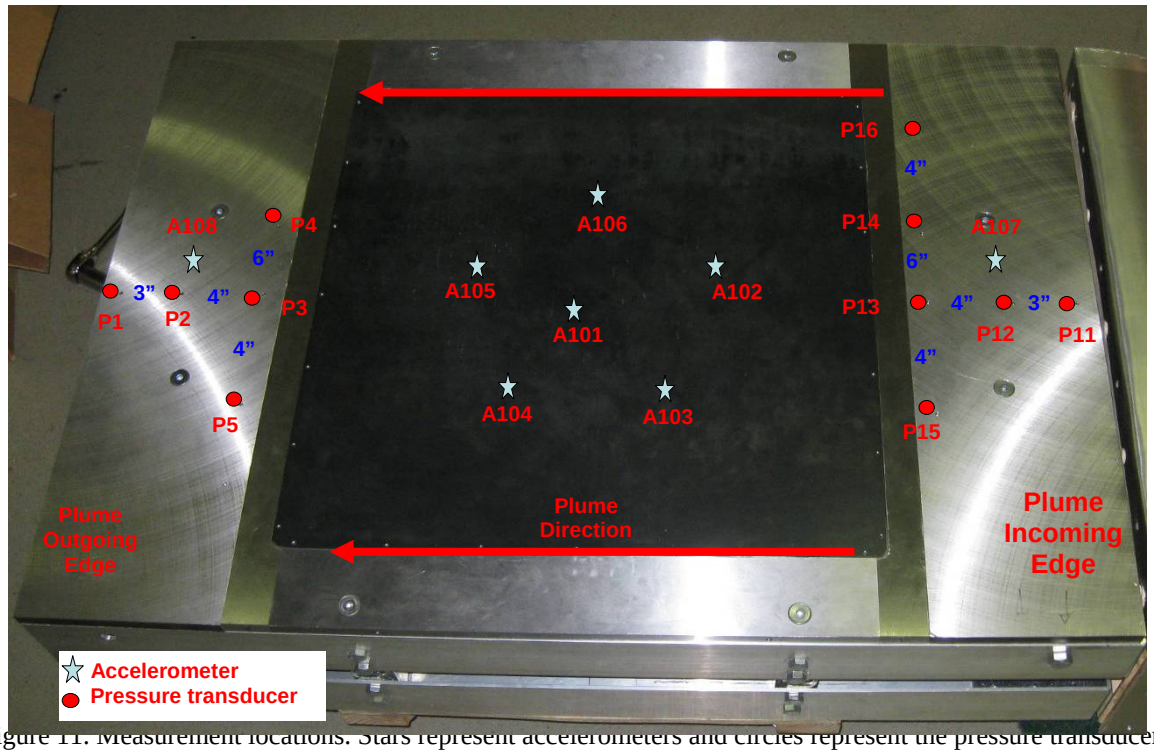

Figure 11. Measurement locations. Stars represent accelerometers and circles represent the pressure transducers.

INSTRUMENTATION

This section discusses all of the instrumentation used to complete the test. The instrumentation included the pressure transducers, accelerometers, strain gage bridge amplifiers (for pressure transducers), thermocouples, transducer signal conditioning, data acquisition hardware, and data collection and analysis computers. The details of the test instrumentation used for this test are provided in Table 2.

Table 2. List of instrumentation used for the motor fire test.

Manf.	Part #	Description
B&K	4384-V	Charge accel 10 pC/G, 482 Deg F, 11 gm, 10-32 stud mount, 12.6 kHz
B&K	AO-0122-D-050	Super low noise cable, 16.7 ft, 482 deg F. micro-dot
B&K	AO-0531-D-010	Cable, micro-dot to BNC, 3.3 ft, 158 deg F.
B&K	2647-A	Charge to IEPE with TEDS, 1 mV/pC
B&K	UA-1192	Set of 10 insulating stud mounts, 10-32 UNF, 392 Deg F.
Kulite	XTEH-10L-190-25SG	25 PSI pressure transducer - 10-32 UNF-2A thread. L=.437"
Kulite	XTEH-10L-190M-3.5BARA	50.75 PSI pressure transducer - M5 x 0.8 thread
Omega	5SRTC-GG-K-20-72	Thermocouple - with glass braid insulation - up to 900 Deg F.

Protection from the harsh environment was the key to a successful test. All of the transducer cabling was first covered with fiberglass/nylon insulation that could withstand high temperatures. It was also routed through a cutout in the back of the mounting plate, as shown in Figure 12. A four-inch steel tube was welded to the back of the plate that was used to protect the cables, as shown in Figure 13. PVC pipe was also used for guiding and protecting the cables.

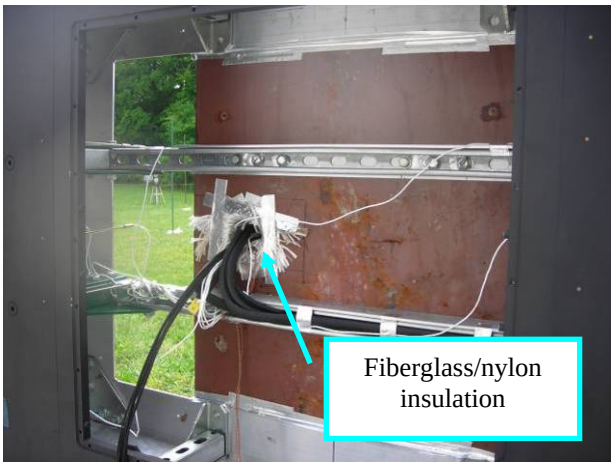

Figure 12. Cables were routed through a hole cut in the back of the mounting plate. These were covered with high-temperature insulation.

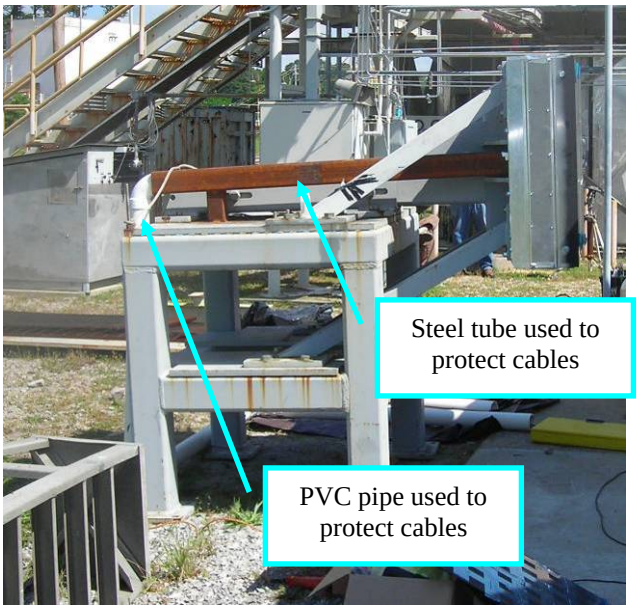

Figure 13. Four-inch steel tube used to insulate cables.

All cables were routed under the steel grid next to the motor and then up through a window into the data acquisition room, as shown in Figure 14 and Figure 15.

Figure 14. Cable routing along the ground.

Figure 15. Cable routing into the data acquisition room.

Accelerometers

The accelerometers installed were high-temperature piezoelectric, charge-style accelerometers made by Brüel & Kjær (B&K), model number 4384. These accelerometer specifications indicate a useful frequency response of 0.1 to 12,500 Hz with a maximum operating temperature rating of 482 degrees F. The nominal sensitivity was 9.8 pC/g. Inline charge to voltage (IEPE) converters (model number 2647-A) were used to power the accelerometers and convert the sensitivity from pC/g to mV/g. PCB model 440 integrated circuit preamplifier (ICP™) signal conditioning units were used to power the accelerometers.

Accelerometers were attached to the sensor plate via 10-32 thread-mounting studs. The 1/8" vibration panel accelerometers were also mounted to ceramic discs used as thermal protection to prevent the accelerometers from getting too hot during the motor firing test. Figure 16 shows an example of the accelerometer installation, including the ceramic discs and cable insulation.

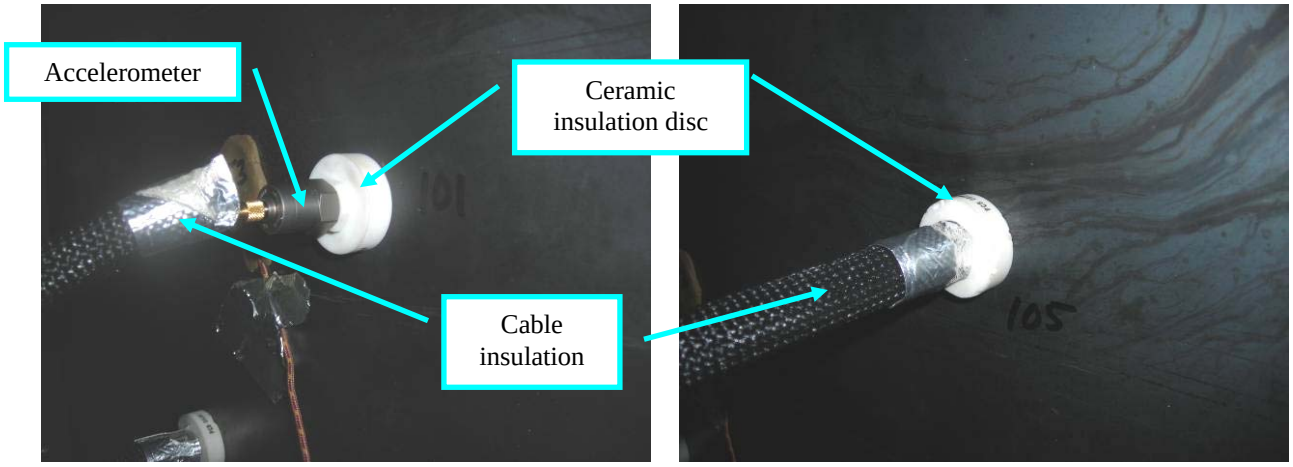

Figure 16. Example accelerometer installation.

Pressure Transducers

The pressure transducers were high-temperature Wheatstone bridge-style pressure transducers made by Kulite, model numbers XTEH-10L-190-25SG and XTEH-10L-190M-3.5BARA. These pressure transducers have a sensing unit with a 6-inch hard line that can withstand 1000 degrees F. They were powered using a VXI 1529 strain gage bridge completion module.

The pressure transducers were attached to the sensor plate via integrated threads, which were either M5x0.8 or 10-32 threads depending on the model (the lead time to acquire enough transducers of the same threading was too short). The pressure plates were machined precisely so that the pressure transducers mounted flush with the front face of the steel plate. Figure 17 shows an example of the pressure transducer installation, including the back side and front side views.

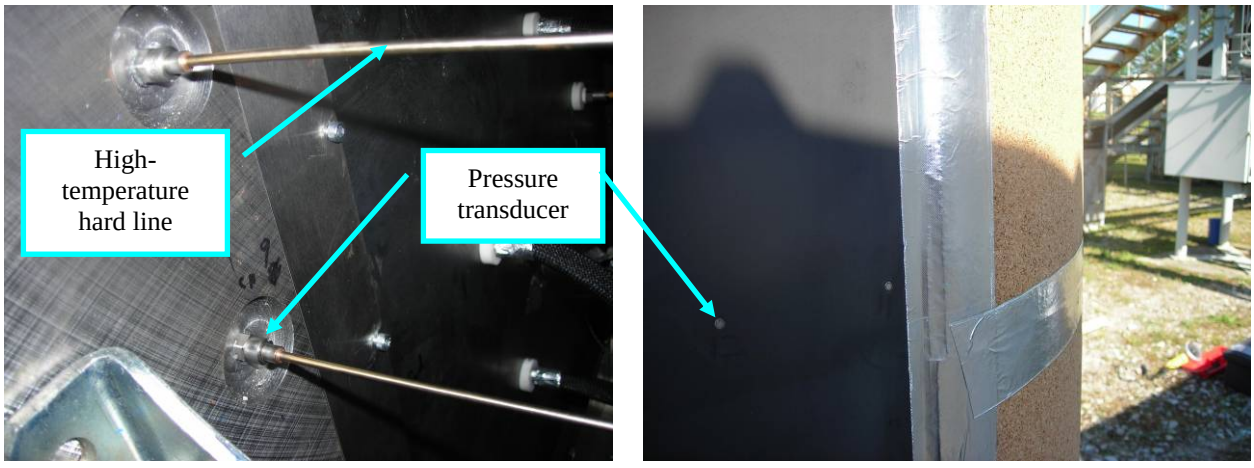

Figure 17. Example pressure transducer installation – back side (left) and front side (right).

Because the phase between the pressure transducers was important, a phase calibration was performed between the pressure transducers at ATA Engineering before the test. The test setup and calibration were valid up to approximately 10,000 Hz. An example of transfer function phase between two of the pressure transducers is shown in Figure 18. The data were used as a reference to verify that there was minimal phase shift between pressure transducers and signal conditioning. This minimal phase shift was within ± 5°, as shown by the upper and lower bounds on the plot.

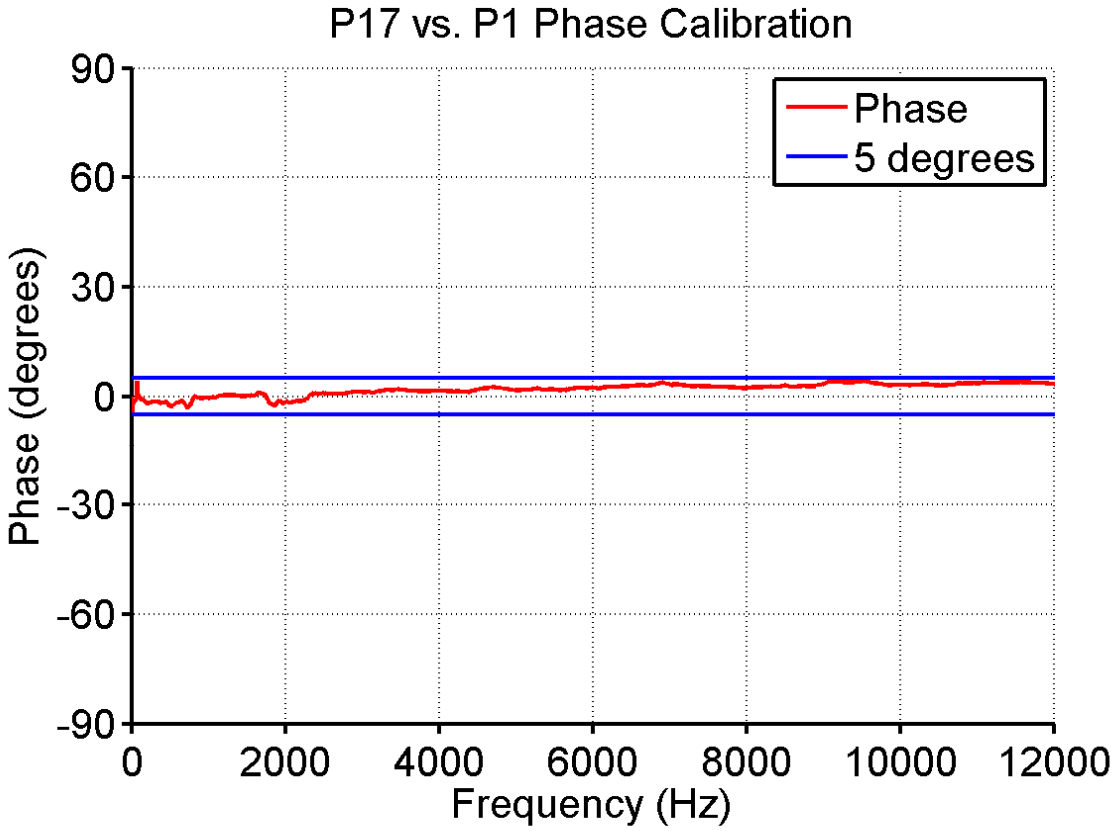

Figure 18. Transfer function phase between pressure transducers 17 and 1.

TEST CONDUCT

The motor firing test was recorded with a sample rate of 65,536 Hz, which resulted in usable data spectral content up to 25,600 Hz. Data were collected for a total of 70 seconds using a VXI Technologies 1432B module. Brüel & Kjær I-deas® Test software and ATA's IMAT™ software were used to acquire and process the data. The time domain data were processed into auto-spectrum for each pressure transducer and accelerometer.

TEST RESULTS

The acceleration and pressure data were recorded for a total of 70 seconds. Data processing was conducted for just the burn event, since this was where all of the relevant data existed. Figure 19

shows a stacked plot of the full time recorded (bottom) for 70 seconds and the cut-out motor firing event (top) from 21.69 to 43.8 seconds.

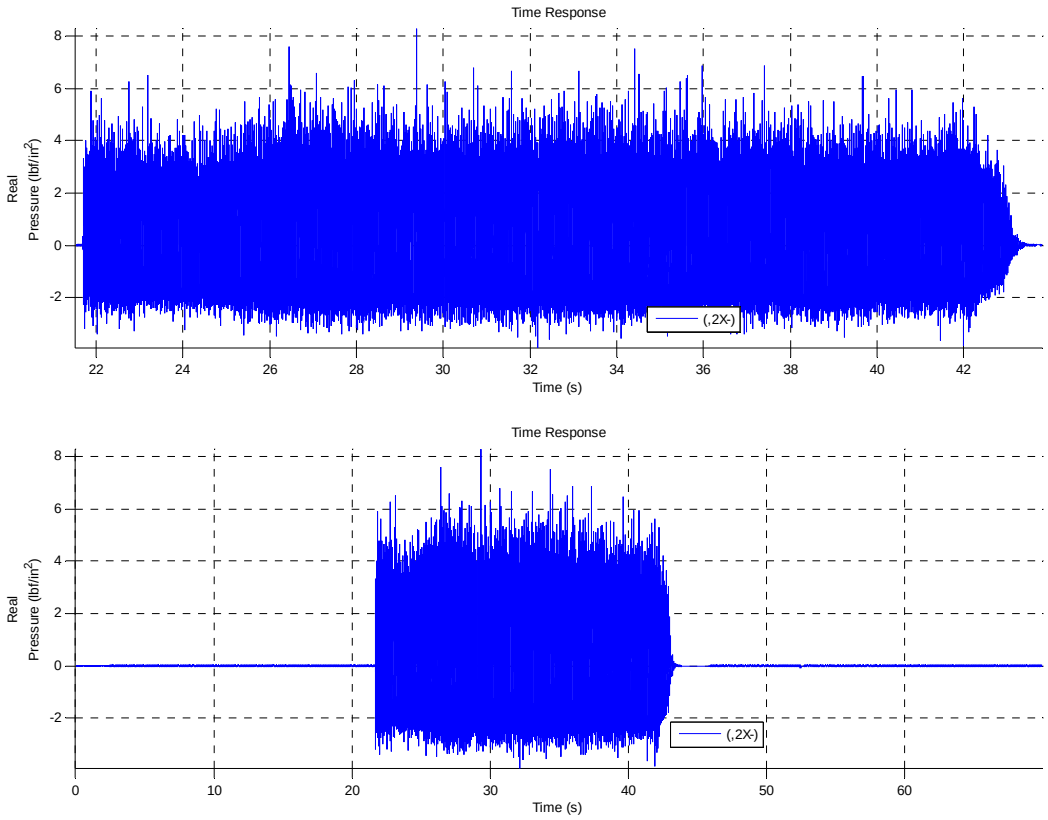

Figure 19. Time history comparison of the full run (bottom) and motor fire event (top).

Temperature Results

The time history plots for the three thermocouples are shown in Figure 20. The temperatures were recorded for a total of 70 seconds. The motor ignition took place at approximately 21.7 seconds and the firing ended at 43.4 seconds. The plots are tagged at the start of the motor burn, at the end of the burn, and at the end of data acquisition. The starting temperatures were approximately 100 degrees F. The temperatures at the end of the burn were 108.7 degrees F on the back surface of the ¾”-thick steel pressure panel, 130.3 degrees F on the front surface of the pressure plate, and 200.3 degrees on the back side of the 1/8”-thick steel accelerometer panel. The temperatures continued to rise after the burn due to the heat transfer through the plate.

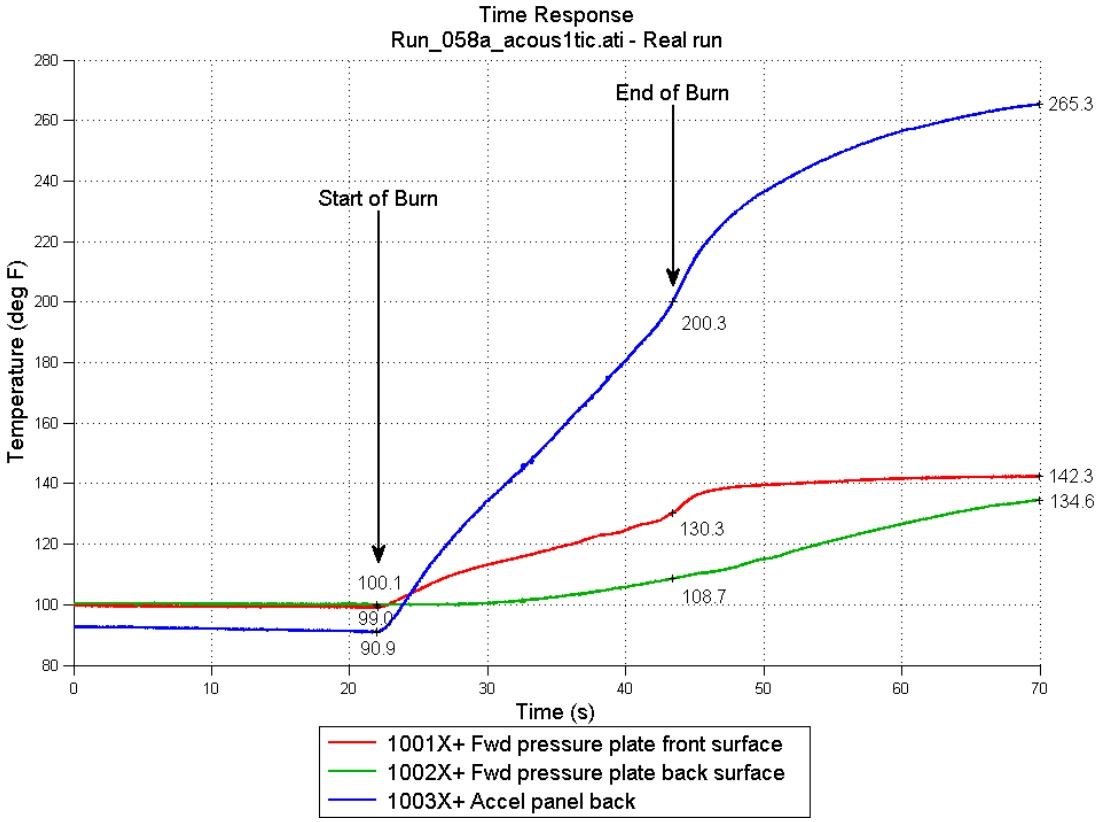

Figure 20. Temperature time history plot for full 70 seconds.

Acceleration Results

The acceleration time data were processed into power spectral densities (PSDs) over the entire time of the motor firing. The PSDs were computed to 25,600 Hz; however, the accelerometer frequency specifications are given as 12,500 Hz for +/- 10% amplitude response. Data presented in this section are from 1 to 12,500 Hz. Table 3 provides the overall root-mean-square (RMS) values for the eight accelerometers. The RMS was computed for the frequency band from 1 to 12,500 Hz.

Table 3. Overall RMS for the accelerometers (G).

Node	Direction	Description	RMS (G)
101	X+	Center	49.94
102	X+	Fwd center	49.38
103	X+	Fwd bottom	47.55
104	X+	Aft bottom	52.34
105	X+	Aft center	56.94
106	X+	Upper	55.57
107	X+	Lead pressure panel	7.76
108	X+	Aft pressure panel	10.39

*Frequency band 1 to 12500 Hz

The aft pressure panel observed higher acceleration levels than the leading panel. It is believed that this is caused by the expanding plume being closer to the aft panel than to the leading panel. A photo of the motor firing with the instrumentation panel is shown in Figure 21. This photo shows how the aft pressure panel is closer to the jet plume boundary layer than to the leading edge.

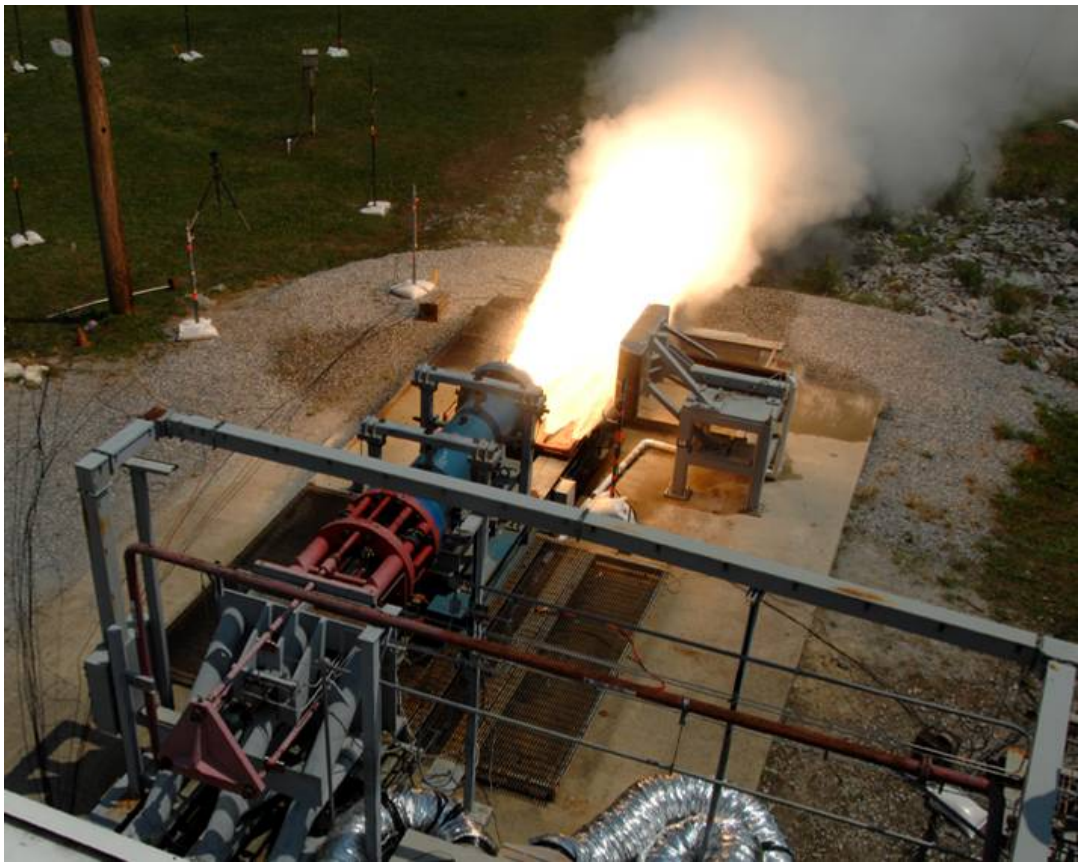

Figure 21. Photo of the motor fire during the burn. (Photo courtesy of NASA MSFC.)

An example time history plot is presented in Figure 22 for the accelerometer mounted to the center of the 1/8” steel panel. The corresponding PSD plot is presented in Figure 23. An overlay of all eight accelerometer PSDs is provided in Figure 24.

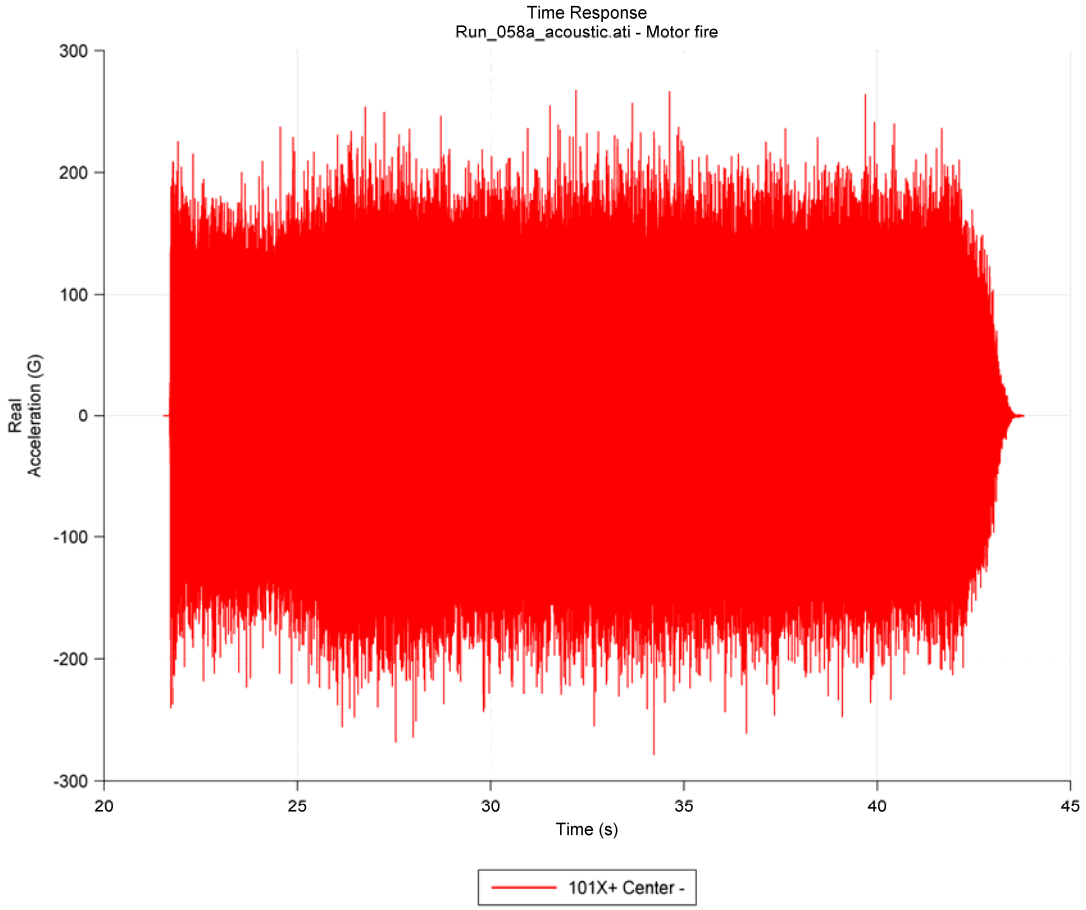

Figure 22. Accelerometer 101X+, center – time history.

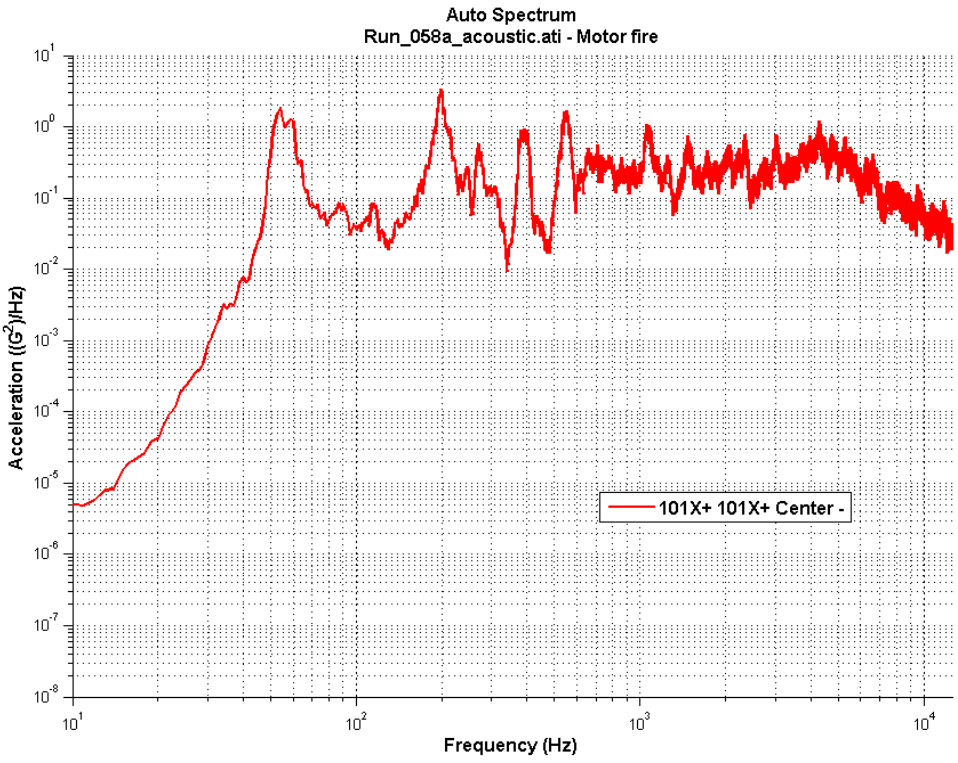

Figure 23. Accelerometer 101X+, center – PSD 49.94 gRMS.

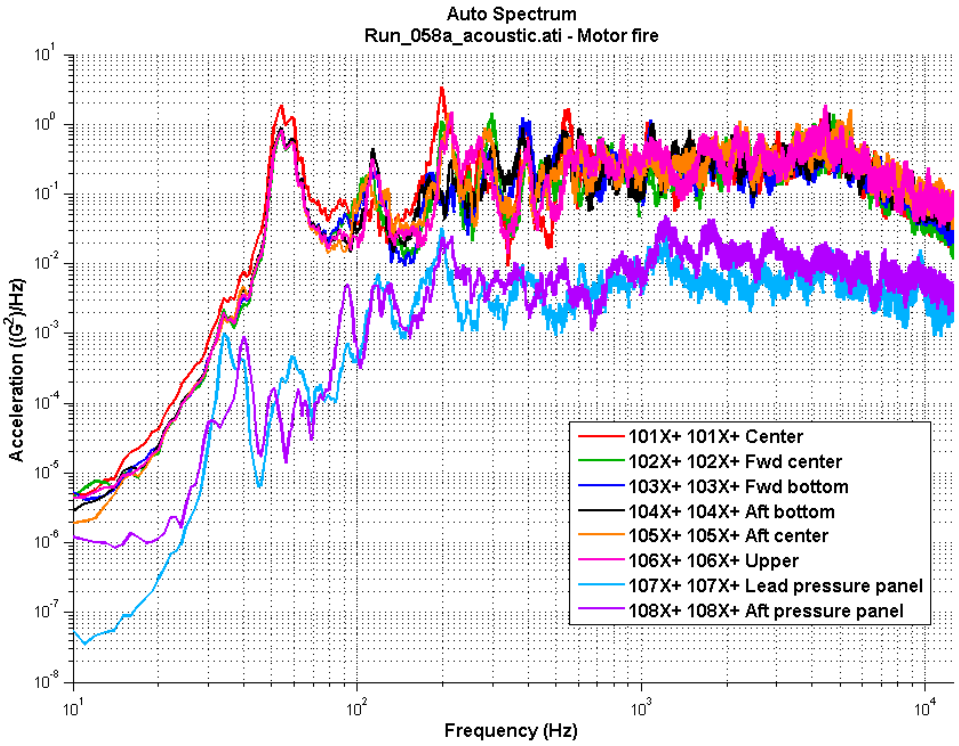

Figure 24. Overlay of accelerometer PSD.

A waterfall analysis was performed on the accelerometer data. The waterfall analysis computes the spectrum for discrete instances (slices) in time and then allows the variation of the spectrum with time to be observed. Here, the data were processed into twenty slices of time with 50% overlap processing, five averages per slice, and a Hanning window applied. A waterfall contour plot for the center panel accelerometer is provided in Figure 25.

The results show that the fundamental vibration mode of the 1/8" accelerometer vibration panel shifts down in frequency as the panel and fixture heat up from the jet plume radiation and as the mass of the hot gas is applied to the panel. The first mode shifts from 66 Hz down to 48 Hz at the end of the burn. Plume gas mass loading of the panel is a possible reason why there is an initial shift in the frequency. The increase in panel temperature could explain the gradual shift in natural frequency over the duration of the firing. Other modes also show shifts in frequency as the panel heats up from the burn. The pressure transducer panels show no shift in vibration frequency as the motor fire continues.

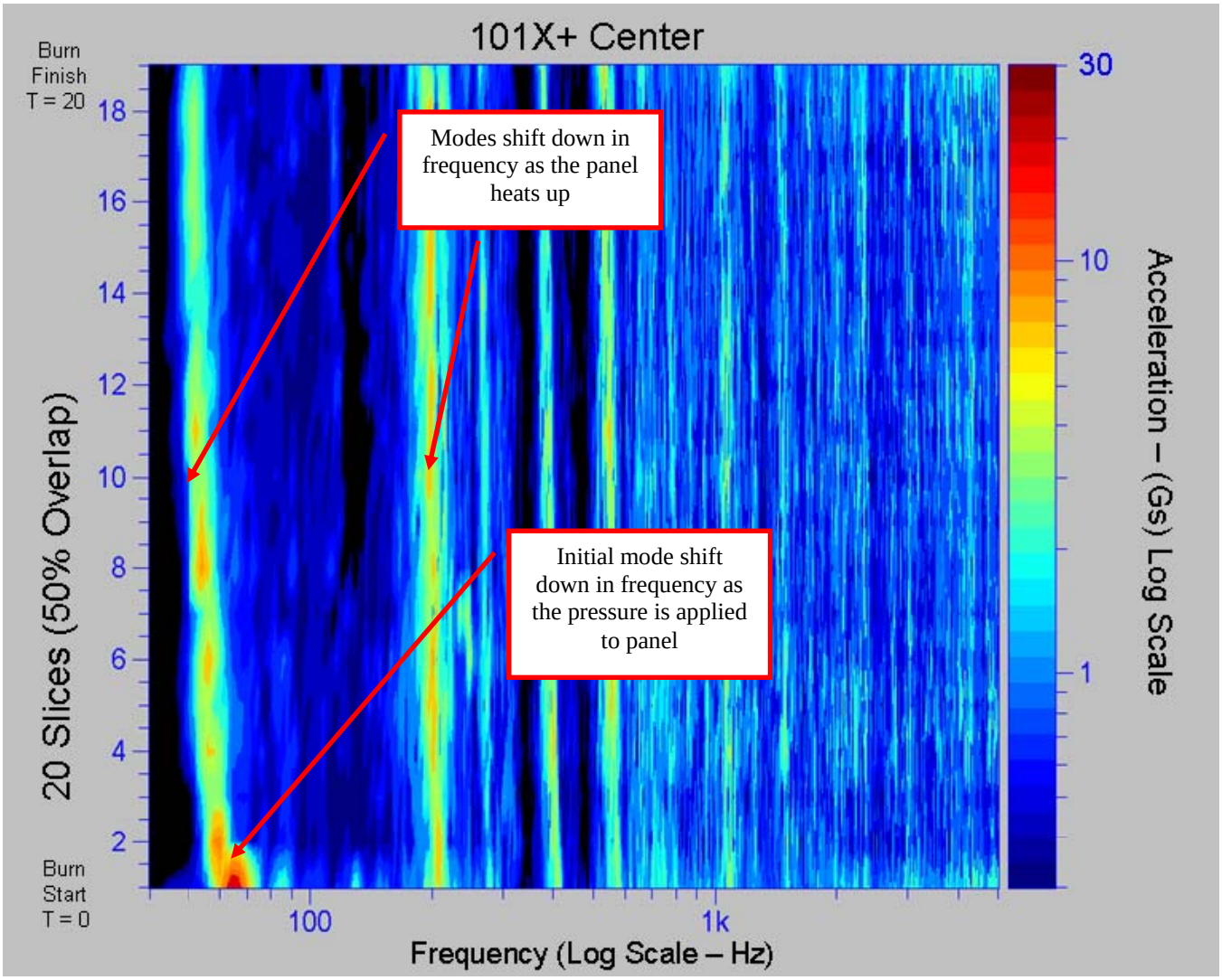

Figure 25. Accelerometer 101X+, center – waterfall contour plot.

Pressure Transducer Results

One of the main goals for this test was to successfully measure the pressure levels without damaging the transducers or cables. ATA was also trying to characterize how the pressure fluctuates in the plume over time and space (relative to each other). The fixed distances between the pressure transducers were important for the phase characterization.

All of the pressure sensors provided quality data for the test. There was one minor anomaly recorded on two of the twelve pressure sensors: Several electrical spikes occurred during the motor fire. The hard line on the back of one of these transducers was bent slightly during installation. The electrical noise and spikes were likely due to a bad cable connection or grounded transducer. The PSD of these responses did not change when comparing them with and without the electrical spikes included in the calculation.

The other nine pressure sensors provided excellent data. The pressure time data were processed into PSDs over the entire time of the motor firing. Cross spectra and transfer functions between all of the pressure sensors were also computed and used in analytical models, but the presentation of these results is beyond the scope of this paper.

The time history plots are presented for a representative pressure transducer in Figure 26 and for sensor 11, which had electrical noise, in Figure 27. The electrical spikes on pressure transducer 11 are called out in the figure. The time domain data show that the fluctuating pressure field is a broadband random process, statistically stationary and of consistent level throughout the 21-second burn. Peak pressures reach near 8 or 9 psi during short instances; however, the aft panel transducers typically measured 6 psi peaks throughout the burn. The leading panel transducers consistently reached 4 psi throughout the burn. The RMS values were computed and were approximately 0.6 psi on the leading panel and 1.0 psi on the aft panel. Inside the instrumentation box, the RMS level was 0.02 psi. Table 4 provides the overall RMS values for the pressure transducers. The RMS was computed from 1 to 25,600 Hz.

The pressure transducers were processed into PSDs, which were computed to 25,600 Hz. Table 4 provides the overall sound pressure levels (OASPL) computed for the twelve pressure transducers. The OASPL were computed using 2.9 e -9 psi (2e-5 Pa) as the dB reference.

The OASPL show that the leading pressure panel was approximately 3.5 to 4 dB lower than the aft panel. This is likely due to the shape of the expanding plume. The leading pressure panel is closer to the nozzle exit, but the aft panel is closer to the edge of the expanding jet plume boundary, which is similar to the acceleration response. The photo previously presented in Figure 21 shows that the aft panel is closer to the edge of the plume due to the plume angle.

A typical PSD plot is presented in Figure 28 for one of the twelve pressure transducers. The last set of data produced and reported is the 1/3-octave band plots of the pressure transducers. Figure 29 provides the aft pressure panel transducer 1/3-octave results and OASPL. Figure 30 provides the leading pressure panel transducer 1/3-octave results. The 1/3-octave band upper center frequency was 20,000 Hz.

Table 4. Overall RMS (psi) and sound pressure level (dB) for the pressure transducers.

Node	Direction	Description	*RMS (PSI)	**OASPL (dB)
1	X-	Aft panel aft	0.98	170.5
2	X-	Aft panel mid	1.01	170.8
3	X-	Aft panel fwd	0.97	170.4
4	X-	Aft panel top	0.99	170.6
5	X-	Aft panel btm	0.93	170.1
11	X-	Lead panel fwd	0.55	165.5
12	X-	Lead panel mid	0.60	166.2
13	X-	Lead panel aft	0.64	166.8
14	X-	Lead panel top	0.66	167.0
15	X-	Lead panel btm	0.64	166.8
16	X-	Lead panel upper top	0.69	167.4
17	X-	Inside box	0.02	137.7

*Frequency band 1 to 25,600 Hz

**dB ref: 2.9e-9 psi

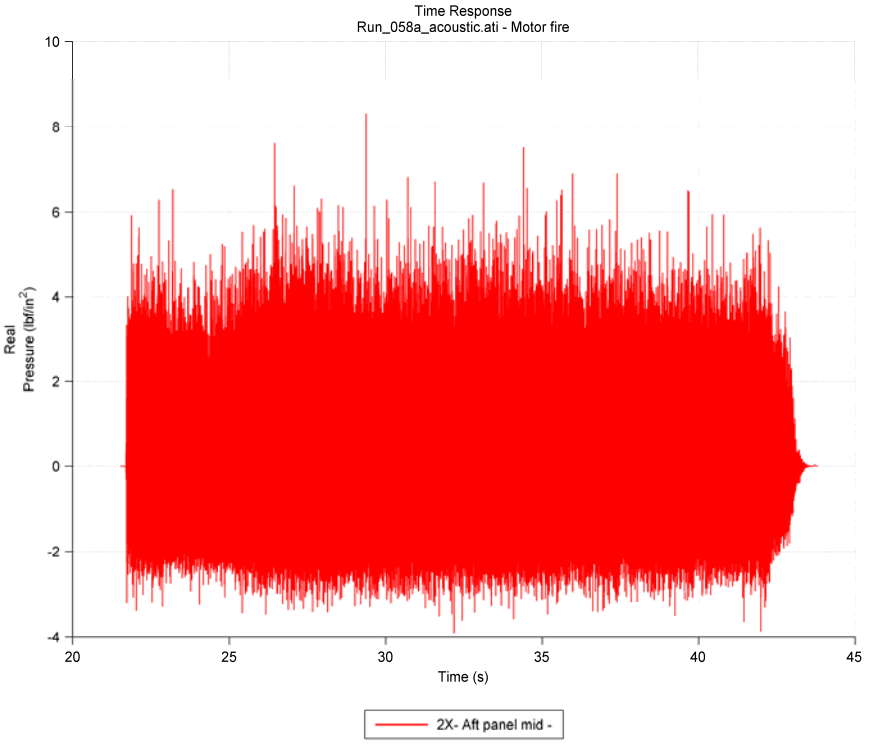

Figure 26. Time response pressure 2 – aft panel middle.

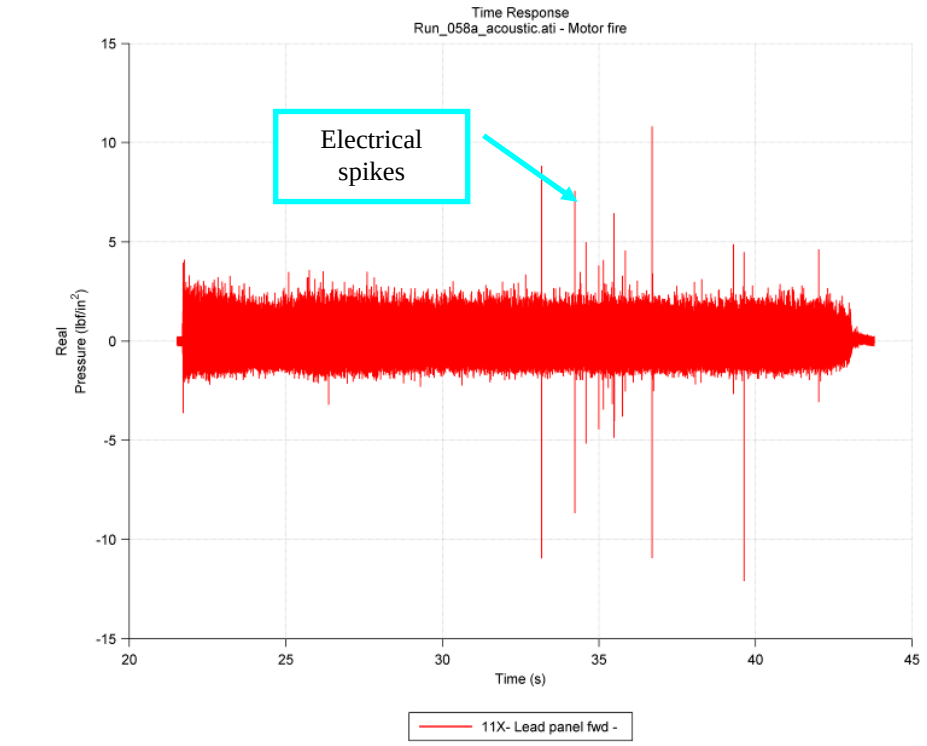

Figure 27. Time response pressure 11 – lead panel forward. The only anomaly that occurred during the test was electrical spikes on two of the twelve pressure sensors.

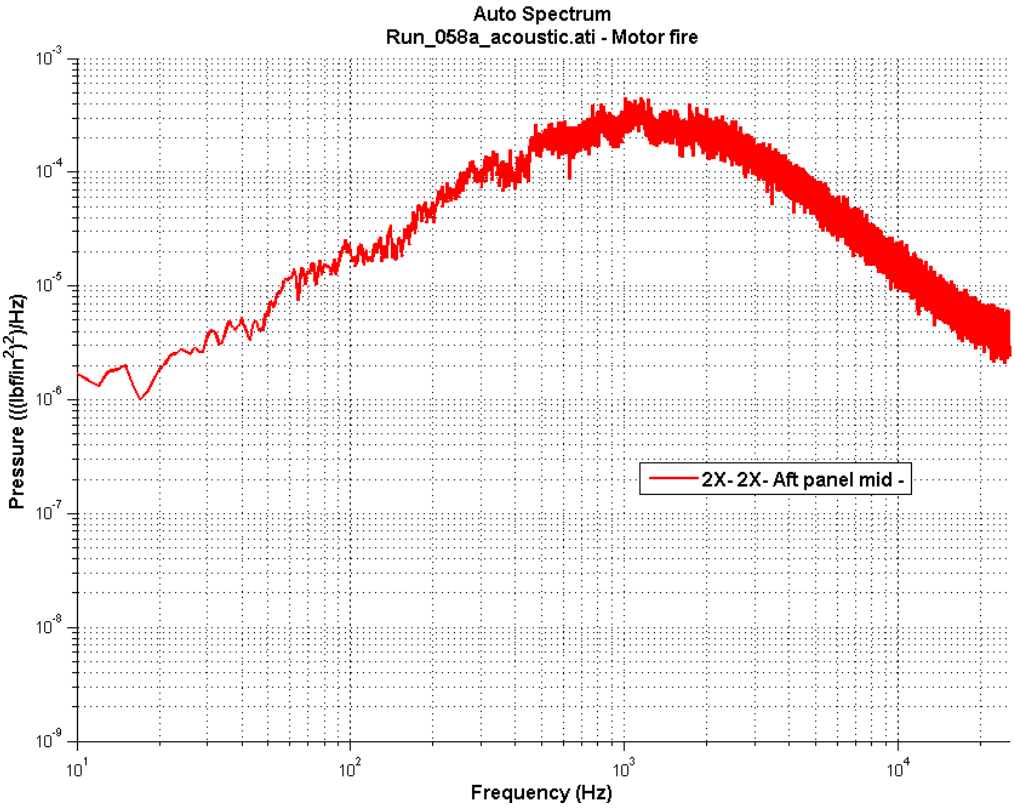

Figure 28. PSD pressure 2 – aft panel middle; 1.01 psi RMS.

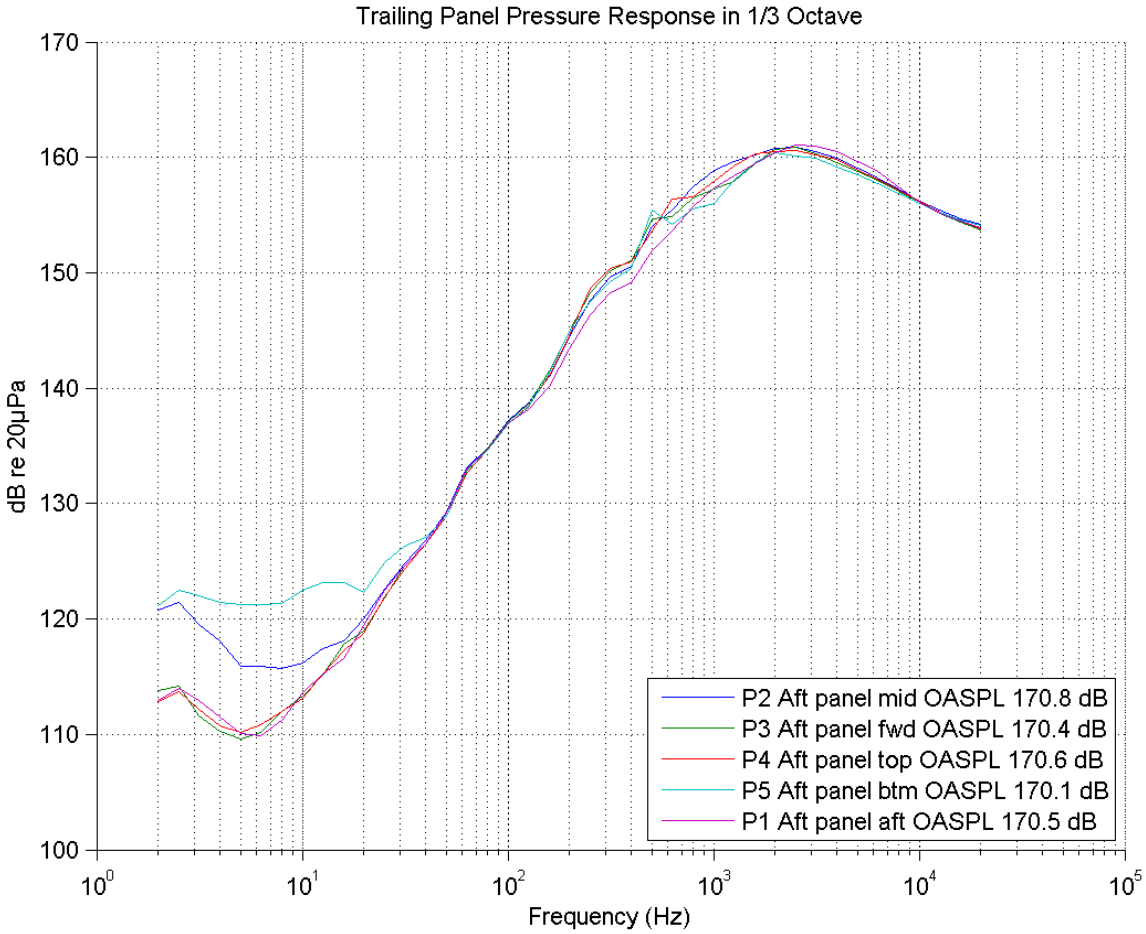

Figure 29. 1/3-octave pressure results for aft pressure panel transducers 1 through 5; OASPL are provided in the figure.

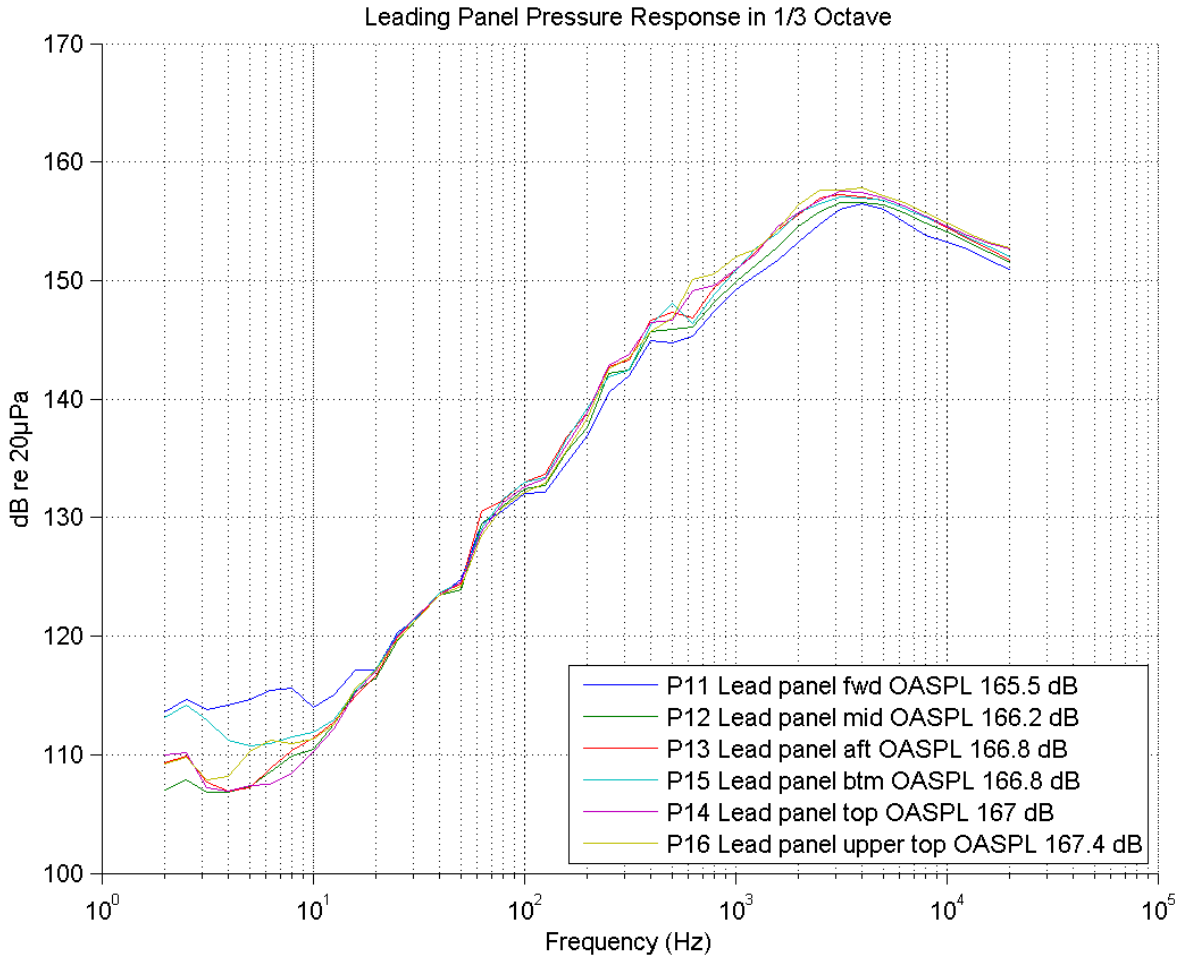

Figure 30. 1/3-octave pressure results for leading pressure panel transducers 11 through 16; OASPL are provided in the figure.

CONCLUSIONS

The plume impingement aeroacoustic and vibration test was successfully performed, with a very short amount of time allowed (less than thirty days) for designing, planning, procuring instrumentation, and manufacturing the instrumentation panels/box. The success of the test was primarily due to designing a test panel and instrumentation set that could survive the high temperatures and pressures in the jet plume; selecting robust instrumentation; and providing adequate protection of the cables.

Measurement of the dynamic fluctuating pressures in the jet plume provided data that will help support future analysis in this type of environment. Measurement of the panel vibration provided a benchmark that can be used to help validate response predictions when applying the fluctuating pressure load cases. This should lead to improvements in the methodology and predictive abilities for future analyses. The OASPL show that the leading pressure panel was approximately 3.5 to 4 dB lower than the aft panel. This is likely due to the shape of the plume. The leading pressure panel is closer to the nozzle exit, but the aft panel is closer to the edge of the jet plume

boundary. The OASPL of the leading edge were near 167 dB, while the aft panel pressures were near 170.5 dB.

Detailed analysis using this test data was also performed by ATA Engineering; this is beyond the scope of this paper and will be published at a later date.

All parties involved with this test program were thrilled that the test was successful. This test program provides an excellent baseline for future testing and for measuring pressures and vibration responses in a jet plume. The actual LAS motor firing is one of the tests planned in the near future that could utilize the concepts and procedures developed in this program.

BIOGRAPHIES

Douglas Osterholt is a graduate from the University of Cincinnati with a Bachelor and Master of Science in mechanical engineering. His studies at the Structural Dynamics Research Laboratory helped prepare him to become one of the lead test engineers at ATA Engineering, where he has specialized in dynamic testing for the past ten years. He has been an author/co-author on a variety of papers published at IFASD, IMAC, and ATS.

Douglas Knox is a graduate from the University of Wisconsin-Madison with a Bachelor of Science in engineering mechanics. His expertise is in dynamic testing, including fatigue, vibration, acoustic, and modal. Currently, Mr. Knox is a test engineer at ATA Engineering, Inc.